**Journal of the Civil Engineering Forum, September 2023, 9(3):263-276**
DOI 10.22146/jcef.6266
Available Online at https://jurnal.ugm.ac.id/v3/jcef/issue/archive

# Seepage Analysis and the Reservoir Water Pollution Potential under Vertical Dam Structure Planning

**Dinar C. Istiyanto, Ika Wulandari*, Shafan A. Aziiz, Rizaldi C. Yuniardi, Suranto, Yofan T.D. Harita, Affandy Hamid, Aloysius B. Widagdo**
National Research and Innovation Agency, Hydrodynamics Technology Research Center, Yogyakarta, INDONESIA
Jalan Grafika No 2 Yogyakarta
*Corresponding author: ikaw001@brin.go.id

**SUBMITTED** 27 November 2022 **REVISED** 25 April 2023 **ACCEPTED** 13 May 2023

**ABSTRACT** A prospective resolution to the intricate predicaments of flooding, sanitation, and the availability of unprocessed water for the populace of Jakarta residents is the implementation of the coastal reservoir paradigm. This paradigm entails harnessing the latent capacity of the Cisadane River flow and its subsequent storage within a retention pond, and then subjecting it to reprocessing to serve as a viable source of raw water. The selection of a vertical seawall design was based on the objective of creating an effective barrier between the reservoir and the sea, while also considering several environmental factors. This design was selected with the aim of minimizing the need for extensive soil excavation and rock placement. However, it is important to note that the risks of construction failure associated with seepage under hydraulic structure and dam stability pose significant challenges. Besides preventing saltwater intrusion and maintaining the integrity of the reservoir as a freshwater source, dam must be designed to mitigate potential seepage failure and intrusion issues. To address these concerns, this study employed numerical simulation using the SEEP/W and CTRAN/W software. The simulation was carried out to analyze seepage discharge under a vertical dam and predict potential seawater intrusion into the reservoir. The dam was examined over a ten-year period, with varying embankment widths of 10m, 20m, and 30m. The analysis considered changes in water level (ΔH) and the addition of a cut-off wall at depths of 5m, 10m, and 15m. The obtained results showed that seepage discharge rates amounted to $3{,}14 \times 10^{-4}$ $m^3$ $s^{-1}$, $2{,}67 \times 10^{-4}$ $m^3$ $s^{-1}$, and $2{,}50 \times 10^{-4}$ $m^3$ $s^{-1}$ for embankment widths of 10m, 20m, and 30m, respectively, under a 1m level difference condition. Following this, the safety factor for piping on vertical embankment was determined as 1.10, 1.34, and 1.39 for widths of 10m, 20m, and 30m, respectively. This factor was found to increase to 4.03 when the embankment distance was widened, and a 15m deep cut-off wall was installed. It is important to note that the seawater intrusion model predicted a seawater concentration of 65,12 g $m^{-3}$ at the bottom for an embankment width of 10m, while no intrusion was observed at widths of 20m and 30m with ΔH=1m. This study aims to assess potential risks of piping due to seepage and seawater contamination at the Cisadane Estuary.

**KEYWORDS** Seepage; Intrusion; Exit Gradient; Cut-Off Wall; SEEP/W



## 1 INTRODUCTION

The Provincial Government of DKI Jakarta and its surrounding areas are currently facing significant challenges related to flooding, sanitation, and raw water supply. These challenges are exacerbated by the impacts of climate change, including increased runoff due to heavy rainfall, decreasing groundwater levels, and rising sea levels that contribute to worsening floods that cannot be easily mitigated. According to projections, the sea level is expected to rise by 50 cm in 2040 compared to 2000, hence, emphasizing the urgency of addressing these issues (Bappenas, 2019). Moreover, the city of Jakarta is also experiencing subsidence, as indicated by the subsidence modeling and microgravity data analysis, revealing a decrease of 8 to 13 cm in areas such as West and North Jakarta (Minardi et al., 2014). This subsidence further compounds the challenges faced by the region. In addition to the problems of flooding subsidence, ensuring an adequate supply of clean water is a growing concern. Access to clean water is essential for sustaining human life and supporting national development. However, the demand for raw water is increasing due to population growth and rapid industrialization, while the availability of freshwater infrastructure is inade-

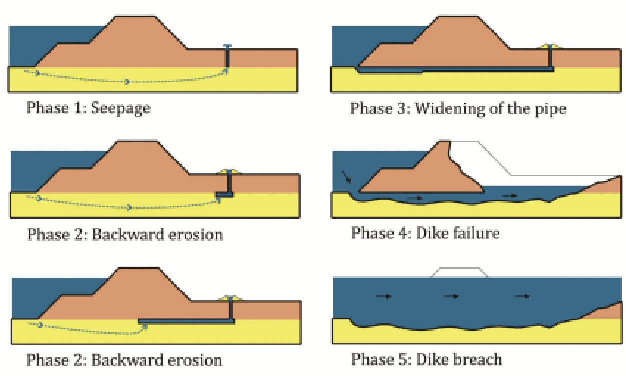


Figure 1 Piping failure mechanism (van BeeK, 2015)

quate. This imbalance leads to excessive exploitation of land resources to meet water needs, which can result in land subsidence and intrusion of seawater into freshwater sources (Kementerian PUPR, 2020). The issue of seawater intrusion is further exacerbated by the global warming-induced rise in sea levels. This rise can disrupt the natural pressure balance in coastal aquifers, causing the interface between groundwater and seawater to shift towards the mainland. As a consequence, groundwater becomes contaminated by seawater, posing a serious threat to its quality and usability (Woo et al., 2019)

The Ministry of National Development Planning (BAPPENAS) is currently implementing a solution to address the challenges of flooding and the need for raw water in Jakarta. This solution involves the construction of the coastal reservoir concept, utilizing the potential of the Cisadane River, and storing water in a retention pond for subsequent reprocessing, thereby making it a source of raw water. The coastal reservoir concept entails the construction of dam on the beach, creating water storage system that serves multiple purposes. One part of the reservoir was designed to collect and store flood water, thereby effectively mitigating the impact of flooding. The other part acts as a collection point for river water, which is then processed and utilized as a source of raw water. Furthermore, BAPPENAS has already planned the construction of a pilot plant for the coastal reservoir, with dam located at the Cisadane estuary (Permadi et al., 2019). Various design plans have been proposed by different stakeholders for the embankment structure of the reservoir, including the implementation of vertical seawall. The choice of vertical seawall design was driven by several considerations, including environmental friendliness and the reduction of extensive soil excavation and rock placement. Therefore, this study aims to examine the stability of vertical embankment structure with different variations in the embankment widths of less than 30m.

Seepage analysis is a crucial consideration when designing vertical barriers to prevent water seepage through or under dam. Several studies have successfully utilized the finite element method to evaluate seepage and stability in earth-fill dam (Athani et al., 2015), clay substitute material as core layers in earth dam type to reduce seepage (Alzamily and Abed, 2022), and computational modeling for seepage prediction in bending conditions (Parsaie et al., 2021). In the case of concrete dam (Elliotis, 2019), various investigators have employed mathematical models to analyze steady-state seepage and evaluate seepage stability (Kasama et al., 2020) in rubble mounds under caisson structure exposed to tsunami overflow and seepage flow. Additionally, Saleh (2018) and Zhang et al. (2021) observed seepage phenomena in reinforced concrete dam foundations using a finite element method that was based on an artificial neural network model with variations in pile depth and grouting location.

Seepage, in this context, refers to the flow of fluids, such as water or oil, through interconnected soil pores, typically moving from areas of higher energy to lower ends. Seepage-related issues pose significant risks to dam construction, accounting for a substantial 50% of construction failures (Fry, 2016). In planning, seepage analysis plays a vital role in slope stability assessment and groundwater pollution control. Typically, the allowable seepage discharge is limited to 1% of the annual average runoff. Failure can occur when seepage amount exceeds this threshold, and this can be influenced by factors such as flow velocity, uplift pressure, and exit gradient (Abokwiek et al., 2022). It is important to note that the water flowing under dam exerts uplifting forces that may lead to cracks and structural failure if the gravity of the structure cannot withstand them. In addition, when exit gradient value surpasses a critical threshold, it can erode soil particles from the foundation, creating voids beneath dam. In this condition, seepage flow can cause internal erosion to initiate piping on dam body and foundation. This seepage flow-induced internal erosion can initiate piping, a phenomenon shown in Figure 1. To mitigate such risks, cut-off wall play a vital role in hydraulic structure design, reducing and controlling uplift forces, seepage discharge, and exit gradient values (Armanuos et al., 2022).

In the process of obtaining raw water to meet the needs of the community, it is crucial to monitor the quality and quantity of water in the reservoir from time to time. Therefore, special attention must be given to the presence of saltwater contamination at the bottom of the reservoir. Seawater intrusion is a form of groundwater pollution (Alcaraz et al., 2015), which occurs when the density of seawater is higher than fresh water. This phenomenon displaces and infiltrates freshwater sources (Purnama and Marfai, 2012). Intrusion of seawater has adverse effects on groundwater quality, reducing the availability of freshwater resources and posing a threat to groundwater reserves (Jacob et al., 1999; Luyun, 2010; Tiyasha et al., 2020). This phenomenon is a major environmental concern in coastal aquifer systems (Klassen and Allen, 2017; Motevalli et al., 2018). In addition, the rising sea levels, as projected by the Intergovernmental Panel on Climate Change (IPCC), are expected to increase further, ranging from 0.52 to 0.98 meters by the end of the century (Stocker et al., 2014; Qutbudin et al., 2019). This condition plays a crucial role in exacerbating seawater intrusion processes. To investigate the impact of distance, height, and head differences of subsurface dam, Chang et al. (2019) conducted a laboratory test using numerical methods. The objective of their study was to gain insights into saltwater intrusion and fresh groundwater discharge. It is also important to note that the effective control of seawater intrusion in multi-layered coastal aquifers has been achieved by implementing cut-off wall (Abdoulhalik and Ahmed, 2017).

This study aimed to determine seepage pattern based on dam width and the differences in elevation between the reservoir water level and the sea level. It also focused on identifying potential piping hazards associated with the design of vertical dam and the spread pattern of seawater contamination in the reservoir over ten years. Furthermore, SEEP/W and CTRAN/W software, as part of the Geo Studio product that has been widely used for studying and analyzing seepage and contamination problems in dam, were employed for this study. Dam design incorporated vertical seawall consisting of vertical concrete panels reinforced with steel rods (Patent Nr. ID0019181 and IDP000071957). These concrete panels measured 220cm in length, 150cm in height and had a thickness ranging from 30cm to 50cm, arranged with bulk material filling between them (Figure 2).

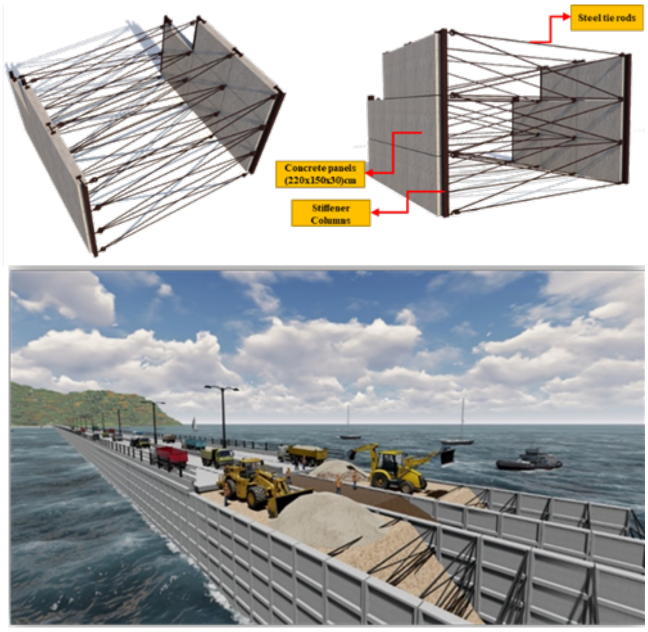


Figure 2 Illustration of the concrete panel with steel rods for seawall construction

## 2 METHODS

This study focuses on the design of vertical seawall using concrete panel wall reinforced with steel rods, incorporating an impermeable layer. The design parameters were determined based on a site survey that considered factors such as planned flood elevation, sea level, and bathymetry. Therefore, the seawall design entailed a height of 10.5 m from a base elevation of -5.00m, with the sea level (MSL) and that of the reservoir water level aligned at ±0,00 m. The wall also incorporated a height of +1.10m and -1.10 m for the High Water Level (HWL) and Low Water Level (LWL), respectively, as shown in Figure 3. The design was further adjusted to meet requirements related to spatial considerations, costs, structural strength, and foundation stability. To explore different design scenarios, the width of dam was varied at 10 m, 20 m, and 30 m, accompanied by cut-off wall with depths of 5m, 10m, and 15m, as shown in Fig-

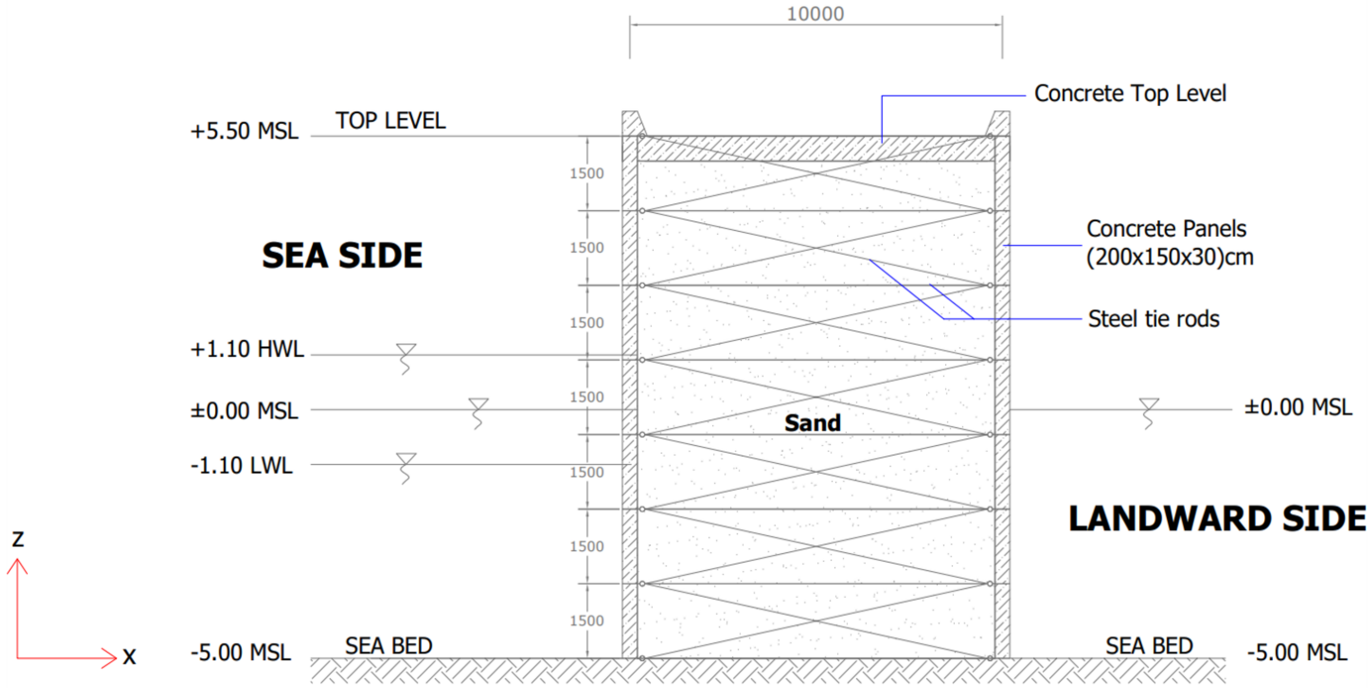


Figure 3 Vertical seawall design plan

ure 4. Following this, numerical simulations utilizing 2D modeling were employed for the sake of calculations, using the finite element method with the assistance of SEEP/W and CTRAN/W software from the Geo Studio 2021.4 suite. These software tools are capable of solving the Laplace Equation by assigning material properties to dam foundation and defining specific boundary conditions, allowing for the determination of hydraulic gradient and seepage discharge rates. It is also important to note that SEEP/W is specifically used to analyze groundwater seepage and excess pore water pressure. Meanwhile, CTRAN/W was employed to model the movement of contaminants through porous materials by using the flow velocity specified by SEEP/W to calculate the movement of dissolved elements within the pores (GEO-SLOPE, 2012*a*,*b*).

Darcy's Law, an equation connecting water flow and porous media, played a crucial role in this study. This equation enables the calculation of flow rates and velocities in saturated soils. The theorem linearly relates the flow through porous media to hydraulic conductivity (k) and gradient of the total hydraulic head (i). Furthermore, it is applicable under steady-state and laminar flow conditions, which can be achieved by modeling the flow with specific constraints such as soil mass, pressure gradient, constant flow, and saturated soil conditions. It is important to note that the formulation of Darcy's Law establishes a linear relationship between specific discharge (Q), Darcian velocity (v), and the cross-sectional area (A), where velocity is the product of permeabilities coefficient (k) and hydraulic gradient (i). The hydraulic gradient, in return, is determined by the elevation differences (ΔH) multiplied by the distance between two points (L).

Following this, Bernoulli's Law was used to evaluate the pore water pressure beneath the groundwater level. This evaluation was carried out by ignoring the velocity factor in the soil $v = 0$, as expressed in Equation 1.

$$h = y + \frac{p}{\gamma} \tag{1}$$

where H is total head energy (m), y is the height of the point relative to a datum (m), p is the pore water pressure at point y (kN $m^{-2}$), and $\gamma$ is the volumetric weight of water (kN $m^{-3}$).

The safety factor analysis was crucial, as it enables proper assessment of the capacity of dam to resist the occurrence of piping hazards. This can be calculated using Equation 2. Therefore, in the design stage, a safety factor value of at least 4 (four) was recommended to account for unforeseen factors,

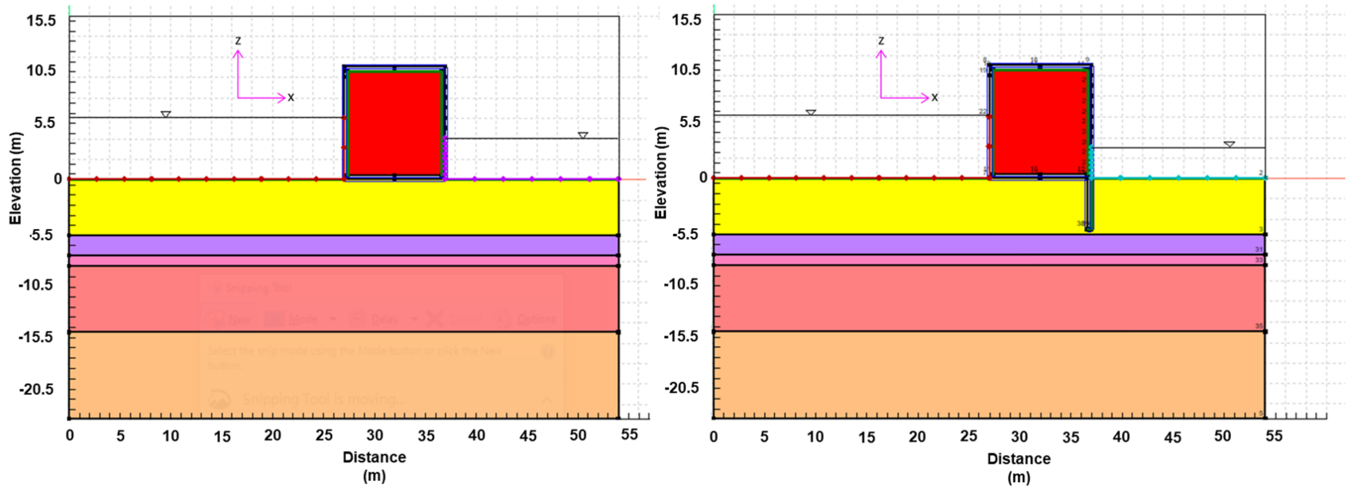


Figure 4 Vertical seawall modeling at 10m width in Geo Studio software a) without cut-off wall b) with cut-off wall

such as soil heterogeneity and degradation over time, ensuring the integrity of dam (Kementerian PUPR, 2017).

$$SF = \frac{I_c}{I_e} \geq 4 \quad (2)$$

$$I_c = \frac{G_s - 1}{1 + e} \quad (3)$$

where $SF$ is a safety factor of piping, $I_c$ is critical hydraulic gradient, $I_e$ represents the permissible to exit gradient, $G_s$ is specific gravity, and e is the void ratio.

The Laplace Law describes the relationship between seepage flow through a homogeneous and isotropic soil material at a steady state. It can be expressed by Equation 4.

$$k_x \frac{\partial^2 h}{\partial x^2} + k_y \frac{\partial^2 h}{\partial x^2} = 0 \quad (4)$$

Following this, the formula for horizontal equivalent hydraulic conductivity is as follows.

$$k_{h(\text{eq})} = \frac{1}{Z} \left( k_{h1}\, dz_1 + k_{h2}\, dz_2 + \ldots + k_{hn}\, dz_n \right) \quad (5)$$

where $k_h$ and $d_z$ are the horizontal hydraulic conductivity and the depth of an individual soil layer, respectively, $k_{h(eq)}$ is the equivalent horizontal hydraulic conductivity, and $Z$ is the total depth.

Table 1. Typical soil permeability coefficient (Carsel & Parrish. 1988)

| Texture | $\theta_r$ | $\theta_s$ | $\alpha$ cm$^{-1}$ | n | K$_{sat}$ m d$^{-1}$ |
|---|---|---|---|---|---|
| Sand | 0.045 | 0.43 | 0.145 | 2.68 | 7.128 |
| Loamy sand | 0.057 | 0.41 | 0.124 | 2.28 | 3.502 |
| Sandy loam | 0.065 | 0.41 | 0.075 | 1.89 | 1.061 |
| Loamy sand | 0.078 | 0.43 | 0.036 | 1.56 | 0.249 |
| Silt | 0.034 | 0.46 | 0.016 | 1.37 | 0.06 |
| Silt loam | 0.067 | 0.45 | 0.02 | 1.41 | 0.108 |
| Sandy clay loam | 0.1 | 0.39 | 0.059 | 1.48 | 0.314 |
| Clay loam | 0.095 | 0.41 | 0.019 | 1.31 | 0.062 |
| Sandy clay | 0.1 | 0.38 | 0.027 | 1.23 | 0.028 |
| Silty clay | 0.07 | 0.36 | 0.005 | 1.09 | 0.005 |
| Clay | 0.068 | 0.38 | 0.008 | 1.09 | 0.048 |

$\theta$_r is residual water content;
$\theta_s$ saturated water contents;
$\alpha$ and n fitting parameters related to particle-size distribution;
$K_{sat}$ saturated hydraulic conductivity.

Meanwhile, seawater contamination can be determined using this basic formula:

$$[K]\,\mathbf{C} = \mathbf{Q} \quad (6)$$

where [K] is the matrix of coefficients related to geometry and materials properties, [C] is the vector of the concentration, and [Q] represents the vector of the contaminant flux quantities.

Table 2. Soil property

| Layer | depth (m) | Soil type |
|---|---|---|
| 1 | 0.0 – 5.5 | Silty clay |
| 2 | 5.5 – 7.5 | Clay |
| 3 | 7.5 – 8.5 | Sandy clay |
| 4 | 8.5 – 15 | Clay |
| 5 | 15 – 23.5 | Silty clay |

Table 3. Soil parameter values based on laboratory test results

| Layer | Soil type | $G_s$ | $e$ | $\gamma$ | $n$ |
|---|---|---|---|---|---|
| 1 | Silty clay | 2.72 | 4.78 | 1.262 | 0.83 |
| 2 | Clay | 2.71 | 4.32 | 1.256 | 0.81 |
| 3 | Sandy clay | 2.71 | 4.32 | 1.256 | 0.81 |
| 4 | Clay | 2.65 | 1.80 | 1.439 | 0.64 |
| 5 | Silty clay | 2.61 | 2.17 | 1.345 | 0.68 |

This study was conducted using secondary soil testing data, which was supplemented minimal and supported by scientific journals and basic standards. These data were processed to derive soil material input parameters for the design process. The initial condition of the base soil of dam was assumed to exhibit a seawater concentration of 0 g m$^{-3}$. Following this, the permeability coefficient values (Table 1) were determined based on soil types, as referenced in Table 2. The soil types and parameters used in this study were obtained from a survey conducted by Dinas Perindustrian dan Energi Provinsi DKI Jakarta in Jakarta Bay water (DKI, 2021), which were presented in Table 2 and Table 3. Table 4 contains the input parameters entered into the software, incorporating the saturated hydraulic conductivity (Table 1) and soil properties (Table 2).

For the subgrade layer of dam design, the soil material used was silt clay soil, which was in accordance with the requirements outlined in SNI 8460-2017 regarding the Geotechnical Design of dam. The specified minimum permeability coefficient value for the subgrade layer was 0,00864 m day$^{-1}$ (BSN, 2017). Moreover, considering the post-reclamation water quality distribution of the North Jakarta Coast in Jakarta Bay Water, with temperatures ranging from 28 - 31 °C, the salinity levels were between 25.42 to 35 g L$^{-1}$ (Kusuma, 2019). It is also important to note that the initial contamination concentration level was assumed to be 0 g m$^{-3}$. The modeling was conducted for a ten-year period, divided into 20 steps, and the boundary conditions applied to the embankment material assumed impermeable characteristics.

Table 4. Soil physical properties for SEEP/W and CTRL/W modeling

| Parameter | 1 | 2 | 3 | 4 | 5 |
|---|---|---|---|---|---|
| Saturated conductivity K (m s$^{-1}$) (in x10$^{-7}$) | 0.58 | 5.56 | 3.24 | 5.56 | 5.56 |
| Saturated water content (m3 m$^{-3}$) | 0.36 | 0.38 | 0.38 | 0.38 | 0.36 |

Table 5. Seepage discharge W=10m

| ΔH (m) | Width 10 m | |
|---|---|---|
| | qf m$^3$ (s m$^{-1}$)$^{-1}$ | Qr m$^3$ s$^{-1}$ |
| 1 | 1.50x10$^{-7}$ | 3.15x10$^{-4}$ |
| 2 | 2.86x10$^{-7}$ | 6.01x10$^{-4}$ |
| 3 | 4.22x10$^{-7}$ | 8.86x10$^{-4}$ |
| 4 | 5.58x10$^{-7}$ | 1.17x10$^{-3}$ |
| 5 | 6.94x10$^{-7}$ | 1.46x10$^{-3}$ |
| 6 | 8.30x10$^{-7}$ | 1.74x10$^{-3}$ |

## 3 RESULTS

### 3.1 Seepage Discharge

From the modeling results above, it can be seen that seepage discharge was calculated using a numerical method with various variations in height differences ($\Delta H$) and dam widths of 10m, 20m, and 30m. The output analysis from the Geostudio SEEP/W software provided seepage discharge per meter width ($q_f$) that flows beneath the foundation of the dam. To obtain the total seepage discharge ($Q_r$), it is necessary to multiply this value by the equivalent cross-sectional width of the dam.

Table 5, Table 6, and Table 7 show that the higher the elevation difference between water in the reservoir and sea levels, the greater seepage discharge.

Table 6. Seepage discharge W=20m

| ΔH (m) | Width 20 m | |
|---|---|---|
| | qf $m^3 (s\ m^{-1})^{-1}$ | Qr $m^3\ s^{-1}$ |
| 1 | $1.27x10^{-7}$ | $2.67x10^{-4}$ |
| 2 | $2.43x10^{-7}$ | $5.10x10^{-4}$ |
| 3 | $3.58x10^{-7}$ | $7.52x10^{-4}$ |
| 4 | $4.74x10^{-7}$ | $9.95x10^{-4}$ |
| 5 | $5.89x10^{-7}$ | $1.24x10^{-3}$ |
| 6 | $7.05x10^{-7}$ | $1.48x10^{-3}$ |

Table 7. Seepage discharge W=30m

| ΔH (m) | Width 30 m | |
|---|---|---|
| | qf $m^3 (s\ m^{-1})^{-1}$ | Qr $m^3\ s^{-1}$ |
| 1 | $1.19x10^{-7}$ | $2.50x10^{-4}$ |
| 2 | $2.27x10^{-7}$ | $4.77x10^{-4}$ |
| 3 | $3.35x10^{-7}$ | $7.04x10^{-4}$ |
| 4 | $4.43x10^{-7}$ | $9.30x10^{-4}$ |
| 5 | $5.50x10^{-7}$ | $1.16x10^{-4}$ |
| 6 | $6.58x10^{-7}$ | $1.38x10^{-4}$ |

## 3.2 Safety Factor

The risk of piping beneath the foundation arises from a downstream seepage flow mechanism, which leads to the formation of piping voids under dam structure. This process typically progresses from downstream to upstream and can ultimately result in dam failure (Griffiths and Fenton, 1993). Additionally, the value of the hydraulic gradient is determined based on the maximum value between the Y-Gradient and XY-Gradient. Exit gradient was evaluated at a distance of 3 m from the downstream point of dam (reservoir side). Figure 5 shows that exit gradient value decreased as dam width was increased with variations of 10m, 20m, and 30m.

Figure 6 presents exit gradient data, revealing a decrease in the number of exit gradient for embankments with widths of 20m and 30m in comparison to dam with a width of 10m. Utilizing

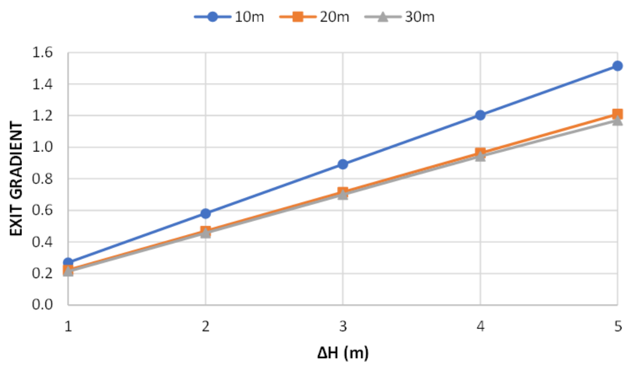


Figure 5 Exit Gradient 10m, 20m, and 30m width

Table 8. Safety factor ΔH=1m

| Width | Type | Exit Gradient | SF |
|---|---|---|---|
| 10 m | without cut-off wall | 0.2694 | 1.10 |
| | cut-off wall 5m | 0.1018 | 2.92 |
| | cut-off wall 10m | 0.0959 | 3.10 |
| | cut-off wall 15m | 0.0841 | 3.54 |
| 20 m | without cut-off wall | 0.2220 | 1.34 |
| | cut-off wall 5m | 0.0876 | 3.40 |
| | cut-off wall 10m | 0.0795 | 3.74 |
| | cut-off wall 15m | 0.0739 | 4.02 |
| 30 m | without cut-off wall | 0.2145 | 1.39 |
| | cut-off wall 5m | 0.0868 | 3.43 |
| | cut-off wall 10m | 0.0833 | 3.57 |
| | cut-off wall 15m | 0.0739 | 4.03 |

Equation 3, the $I_c$ value was calculated as 0,2976, hence, enabling the determination of the safety factor value as follows:

1. For $W = 10\,\text{m}$, the safety factor number is: $SF = \frac{I_C}{I_e} = \frac{0.2976}{0.2694} = 1.1045 < 4$ (not saved)
2. For $W = 20\,\text{m}$, the safety factor number is: $SF = \frac{I_C}{I_e} = \frac{0.2976}{0.222} = 1.3406 < 4$ (not saved)
3. For $W = 30\,\text{m}$, the safety factor number is: $SF = \frac{I_C}{I_e} = \frac{0.2976}{0.2145} = 1.3874 < 4$ (not saved)

Table 8 displays the results of dam safety factor calculations with and without the implementation of cut-off wall.

## 3.3 Cut-Off Wall

Analysis of the safety factor showed that the three dam, with widths of 10m, 20m, and 30m, still exhibited an enormous piping hazard potential. The obtained safety factor value indicated that the observed dam were considerably below the desired safety threshold. However, the introduction of cut-off wall at depths of 5m, 10m, and 15m showed promising results in increasing the safety factor value of vertical dam. Based on the data in Table 8, it is evident that incorporating cut-off wall at an embankment width of 20m and 30m, along with an elevation difference of 1m, can substantially enhance dam's resistance against piping hazards. The resulting safety values for the embankment widths were 4.02 and 4.03, respectively, indicating a significant improvement in dam stability.

## 3.4 Sea Water Intrusion

CTRAN/W software, which was used to simulate and model the movement of seawater through the ground, is shown in Figure 7. The parameters and values obtained from SEEP/W modeling served as the basis for the calculation performed in CTRAN/W. On the other hand, Figure 8 shows the progressive expansion of the seawater spreading pattern of seawater over different periods, specifically 5, 10, 25, and 50 years.

Figure 9 shows how the difference in elevation between the sea level and reservoir, as well as the width of dam, plays a significant role in determining the distribution of saltwater concentrations and seepage exit point on dam. It was observed that dam with a width of 20m or 30m could effectively diminish the saltwater concentration beneath the reservoir within ten years.

Figure 10 shows the impact of installing cut-off wall in the downstream region of vertical dam on the concentration of saltwater beneath the reservoir. The results obtained revealed a significant reduction in concentration with the implementation of a cut-off wall at a depth of 5m. The concentration levels decreased progressively, reaching 94%, 57%, 12%, and 0% at ΔH = 1m, 2m, 3m, 4m, and 5m, respectively. Notably, the depth of cut-off wall correlates directly with the magnitude of the concentration decrease.

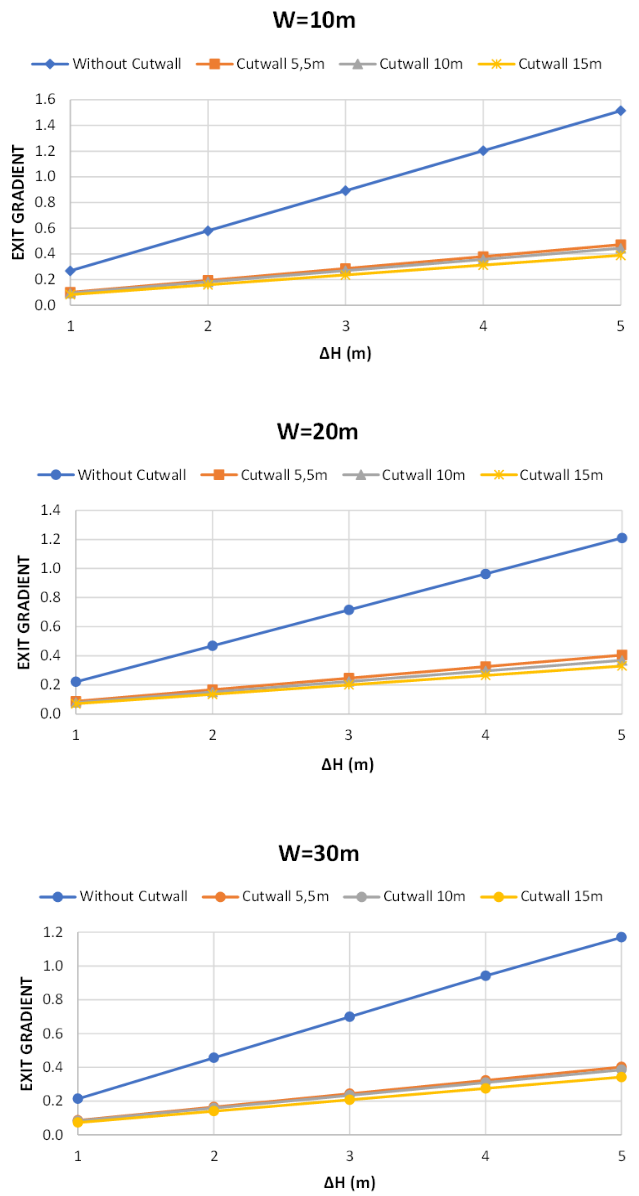


Figure 6 Exit Gradient of dam with cut-off wall

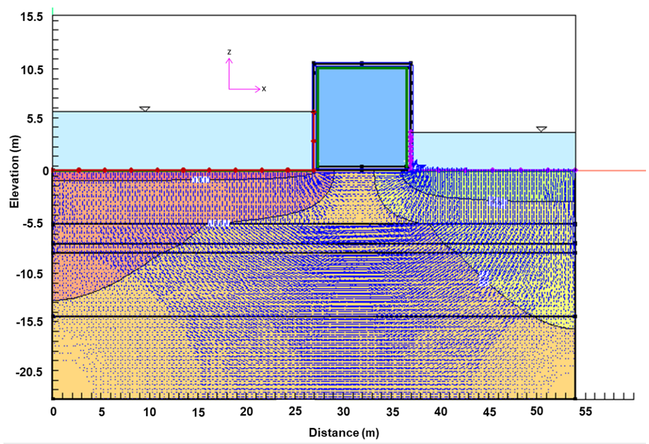


Figure 7 Seawater intrusion flow pattern

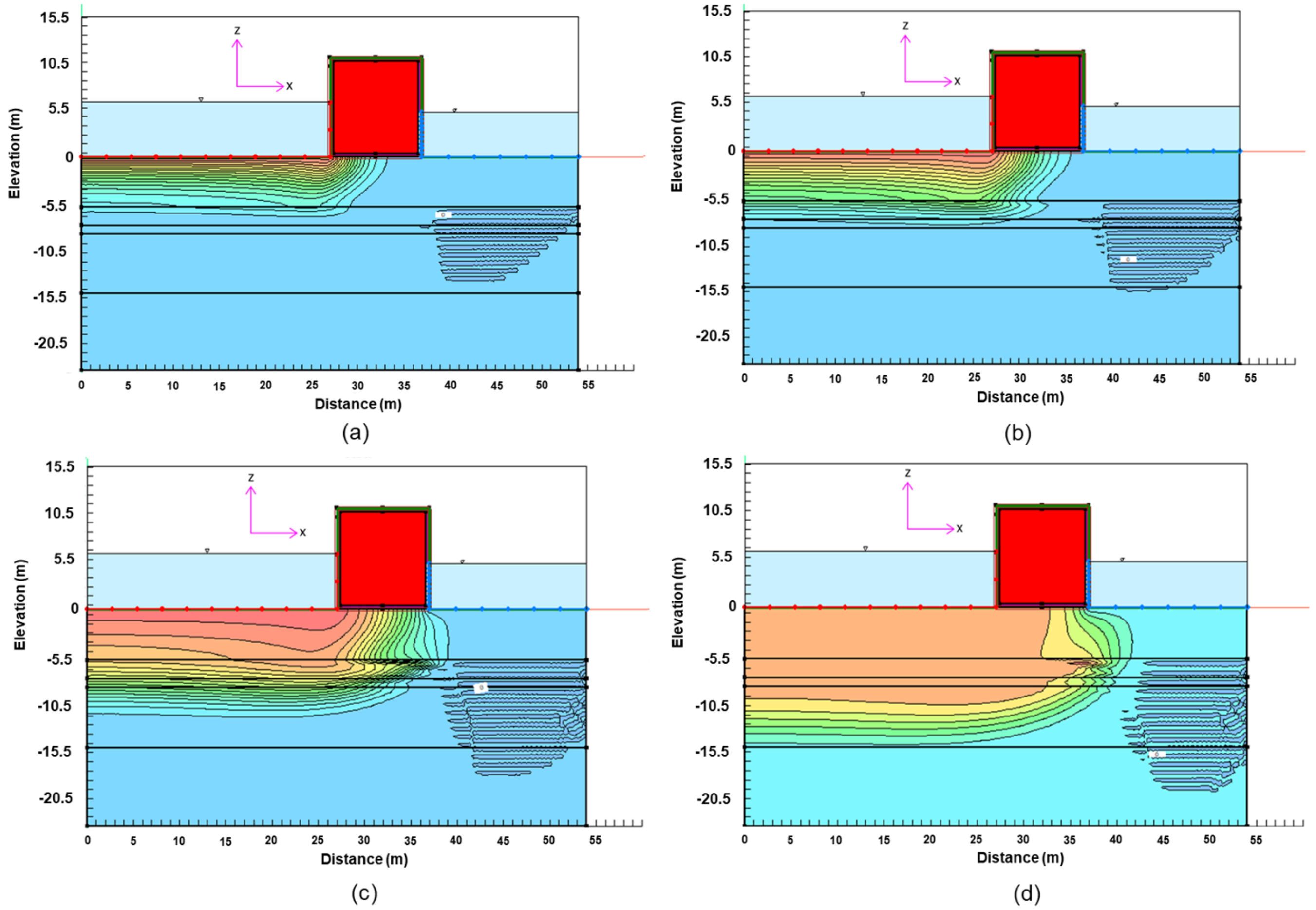


Figure 8 Sea Water Intrusion was modeled with ΔH= 1m in 5, 10, 25, and 50 years.

Table 9. The reservoir bottom salt concentration W=10m in 10 years (g m$^{-3}$)

| | ΔH | | | | |
|---|---|---|---|---|---|
| | 1m | 2m | 3m | 4m | 5m |
| WCW | 65.1 | 323 | 657 | 1.001 | 1.273 |
| CW 5m | 0.01 | 24 | 394 | 1.311 | 1.963 |
| CW 10m | 0.00 | 0.04 | 13 | 200 | 1.748 |
| CW 15m | 0.00 | 0.00 | 0.01 | 1.31 | 30 |

## 4 DISCUSSION

A study conducted by Abokwiek et al. (2022) regarding seepage flow under concrete dam showed that the width of dam was inversely proportional to seepage rate. A 1m increase in the width was found to reduce seepage rate by 3,7%. However, the difference in water level is directly proportional to seepage rate, with a 10% increase observed for every additional 1m of elevation. In this study, dam with different embankment widths of 20m and 30m were analyzed, both of which showed seepage reductions of 15.09% and 20.7%, respectively. The effectiveness of widening dam was greater at 20m compared to 30m. Furthermore, the greater difference in elevation between the reservoir water level and the sea water resulted in a more significant seepage discharge. Seepage discharge increased linearly by 91% for every 1m difference at widths of 10m, 20m, and 30m. Armanuos et al. (2022) stated that the use of q an inclined double cut-off wall is effective in controlling exit gradient and seepage discharge. In line with analysis results, a reduction of 17.61% and 20.39% in seepage was observed for dam widths of 20m and 30m, respectively. In a study conducted by Abdoulhalik and Ahmed (2017) on seawater intrusion using experimental and numerical methods, it was found that the installation of cut-off wall proved effective in reducing seawater content by up to 43%. The study utilized a 15m deep cut-off wall at a 10m wide dam, and this resulted in a

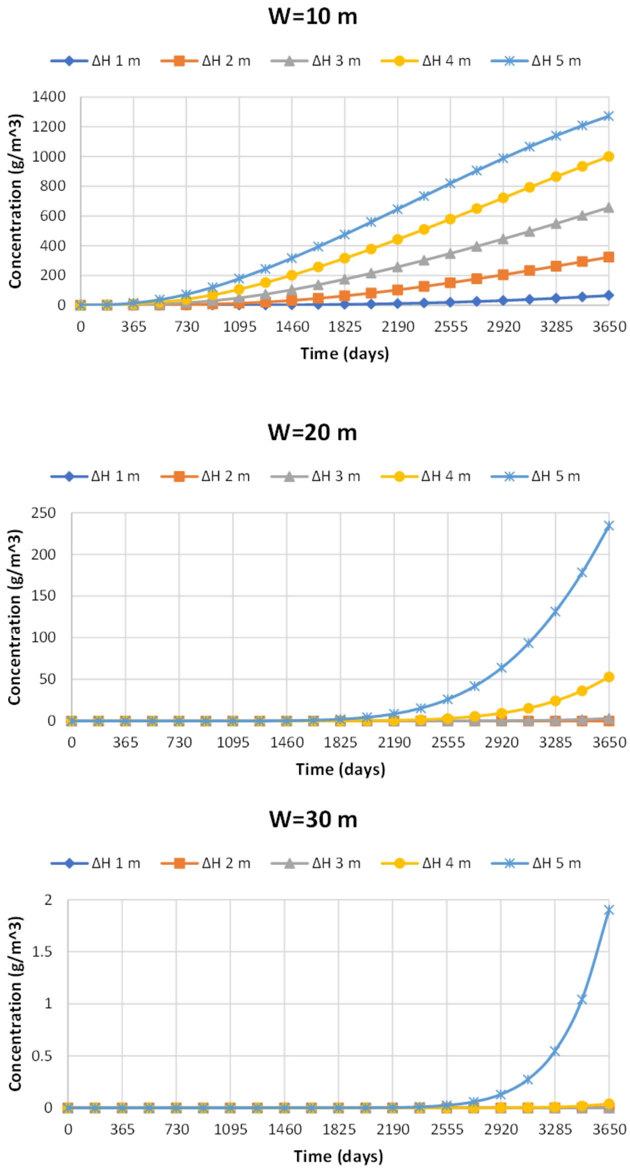


Figure 9 Seawater concentration

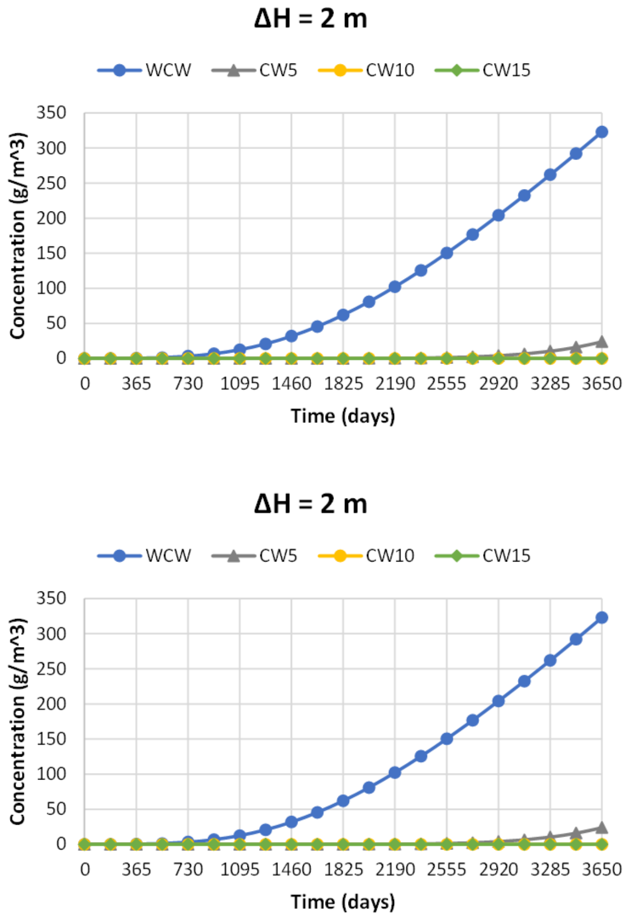


Figure 10 Concentration effect of installing cut-off wall (W=10m)

94% reduction in seawater concentration at a predetermined point.

Based on the soil properties in the field, dam widths ranging from 10m to 30m are considered unsafe for potential piping. In this regard, to ensure a safe safety factor value, a 15m deep cut-off is required for dam widths of 20m and 30m. Notably, the addition of cut-off wall at the bottom of dam effectively reduced the concentration of salt water in the reservoir.

## 5 CONCLUSION

In conclusion, a numeric analysis was conducted in this study to analyze seepage stability under dam and intrusion of seawater into the reservoir. It is important to note that dam failures can occur due to excessive seepage, which is significantly influenced by exit gradient. As a result, seepage analysis and intrusion modeling were carried out based on a study of vertical dam structure using secondary data from the Cisadane River Estuary. Dam widths considered were 10m, 20m, and 30m. The obtained results showed that the width of dam is a significant factor affecting seepage, as shown in Figure 5 . A comparison of dam widths revealed seepage rate decrease of 15.09% and 20.7% for the 20m and 30m widths, respectively, compared to 10m. Notably, the 20m width showed a substantial reduction in the value of exit gradient value, while the effect was less pronounced for the 30m width. In this study, differences in the sea level and the reservoir elevation were observed to have a significant impact on increasing exit gradient value. It was discovered that with each 1m rise in water level, the discharge increased by 91%. This rise in discharge can lead to a decrease in the safety factor of dam, posing potential risk to piping. Following this difference, exit gradient value was found to reduce by 17.61% and 20.39% for dam widths of 20m and 30m, respectively. In addition, the obtained safety factor value fell short of the specified threshold requirements. The safety factor values for dam with 10m, 20m, and 30m widths were determined as 1.10, 1.34, and 1.39, respectively. Given that these values do not meet the necessary safety requirements, the implementation of cut-off wall beneath dam becomes crucial to mitigate seepage discharge and reduce exit gradient value. Table 8 shows the effectiveness of adding cut-off wall to a 10m wide dam in increasing the value of the safety factor. The inclusion of cut-off wall at depths of 5m, 10m, and 15m was found to increase the safety factor values from 1.10 to 2.92, 3.10, and 3.54, respectively. Therefore, the design indicated that for dam widths of 20m and 30m, incorporating cut-off wall at a depth of 15m achieved satisfactory safety factor values of 4.02 and 4.03, ensuring protection against piping hazards.

In addition to the safety factor of a dam, when constructing the reservoir for storing raw water, ensuring water quality is a crucial aspect to consider. Typically, one of the problems that occur in a reservoir located near a sea is seawater intrusion. This intrusion is greatly influenced by the difference in height between the seawater and the reservoir water levels. It was estimated that over a period of 10 years, the height difference could result in a salt concentration increase of up to 20 times at $\Delta H = 5m$ compared to $\Delta H = 1m$.

In this situation, widening dam widths presents a potential solution for reducing salt concentration in the reservoir. It was found that a 20m wide dam can lower the concentration by 81.56%, while a 30m wide dam can achieve a reduction of 99.85%. Following this, in the modeling of seawater intrusion into the dam, the observed salt concentration at the bottom of the reservoir was 65.12 g $m^{-3}$ at $L = 10m$ and 0 g $m^{-3}$ at $L = 20m$ and $30m$ with $\Delta H = 1m$ over a ten-year period. These values indicated that by widening the dam, specifically at widths of 20m and 30m, the seawater concentration can be completely eliminated at a water level difference of 1m. The installation of a cut-off wall proved effective in reducing both the velocity and salt concentration at the bottom of the reservoir.

## DISCLAIMER

The authors declare no conflict of interest.

## ACKNOWLEDGMENTS

This study is supported by The Disaster Technology Research Program of the National Research and Innovation Agency (DIPA BRIN) No 124.01.KB.6693.SDB.001.051.A. The authors are grateful to the management of the Hydrodynamics Technology Research Center, especially the investigators, engineers, lab technicians from the Structural Numerical Modeling Department, and staff who helped make this project a success.

## REFERENCES

Abdoulhalik, A. and Ahmed, A. A. (2017), 'The effectiveness of cut-off walls to control saltwater intrusion in multi-layered coastal aquifers: Experimental and numerical study', *Journal of Environmental Management* **199**, 62–73.

Abokwiek, R. et al. (2022), 'A finite element model for the analysis of seepage flow of water under concrete dams', *Geotechnical and Geological Engineering* **40**, 2823–2841.

Alcaraz, R., Graniel, E., Castro, A. F. and Vadillo, I. (2015), 'Assessment of groundwater contamination in yucatan peninsula (mexico) by geostatistical analysis', *Environmental Earth Sciences* **1**.

Alzamily, Z. N. and Abed, B. S. (2022), 'Experimental and theoretical investigations of seepage reduction through zoned earth dam material with special core', *Material Today* **61**(3), 998–1005.

Armanuos, A. M. et al. (2022), 'Impact of inclined double-cutoff walls under hydrolic structures on uplift force, seepage discharge and exit hydrolic gradient', *Ain Shams Engineering Journal* **13**(1).

Athani, S. S., Shivamanth, Solanki, C. H. and Dodagoudar, G. R. (2015), 'Seepage and stability analyses of earth dam using finite element method'.

Bappenas (2019), *Rencana Pembangunan Jangka Menengah Nasional Tahun 2020 - 2024*, Bappenas, Jakarta.

BSN (2017), 'Sni 8460-2017 persyaratan perencanaan geoteknik'.

Chang, Q. et al. (2019), 'Effect of subsurface dams on saltwater intrusion and fresh groundwater discharge', *Journal of Hydrology* **576**(9).

DKI, P. (2021), Laporan akhir data log bor bh-01, bh-02, bh-03, di teluk jakarta, Technical report, Dinas Perindustrian dan Energi Provinsi DKI Jakarta, Jakarta, Indonesia.

Elliotis, M. C. (2019), 'A mathematical model for a steady-state seepage flow of groundwater under a reinforced concrete dam', *Applied Computing and Geosciences* **1**.

Fry, J. J. (2016), *Lessons on internal erosion in embankment dams from failures and physical models*, s.n., Oxford.

GEO-SLOPE (2012*a*), *Contaminant Modeling with CTRAN/W*, GEO-SLOPE International Ltd., Canada.

GEO-SLOPE (2012*b*), *Seepage Modeling with SEEP/W*, GEO-SLOPE International Ltd., Canada.

Griffiths, D. V. and Fenton, G. A. (1993), 'Seepage beneath water retaining structures founded on spatially random soil', *Géotechnique* **43**(4), 577–587.

Jacob, B. et al. (1999), Seawater intrusion in coastal aquifers concepts, methods and practices, *in* 'Theory and Applications of Transport in Porous Media', Springer Science & Business Media, Berlin.

Kasama, K., Zen, K., Nakagawa, Y. and Furukawa, Z. (2020), 'Instability evaluation of rubble mound for breakwaters subjected to tsunami-induced overflow and seepage flow', *Soils and Foundations* **60**(6), 1532–1545.

Kementerian PUPR (2017), *Modul Analisa Stabilitas Bendungan: Perhitungan Rembesan*, Bandung.

Kementerian PUPR (2020), *Rencana Strategis Direktorat Jenderal Sumber Daya Air Kementerian 2020-2024*, Jakarta.

Klassen, J. and Allen, D. M. (2017), 'Assessing the risk of saltwater intrusion in coastal aquifers', *Journal of Hydrology* **551**, 730–745.

Kusuma, A. H. (2019), 'Sebaran kualitas air pantai utara jakarta pasca reklamasi di perairan teluk jakarta', *Jurnal Teknologi Perikanan dan Kelautan* **10**, 149–160.

Luyun, R. A. (2010), Effects of Subsurface Physical Barrier and Artificial Recharge on Seawater Intrusion, PhD thesis, United Graduate School of Agricultural Sciences, s.l.

Minardi, S., Hiden, Dahrin, D. and Yusuf, M. (2014), 'Analisa penurunan airtanah dan amblesan tanah dengan metode gayaberat mikro dan gradien vertikal antar waktu: Studi kasus di jakarta', *Jurnal Ilmu Dasar* **15**(1), 7–14.

Motevalli, A., Moradi, H. R. and Javadi, S. (2018), 'A comprehensive evaluation of groundwater vulnerability to saltwater up-coning and sea water intrusion in a coastal aquifer (case study: Ghaemshahr-juybar aquifer)', *Journal of Hydrology* **557**, 753–773.

Parsaie, A., Haghiabi, A. H., Latif, S. D. and Tripathi, R. P. (2021), 'Predictive modelling of piezometric head and seepage discharge in earth dam using soft computational models', *Environmental Science and Pollution Research* **28**, 60842–60856.

Permadi, A. S. C. et al. (2019), 'Perencanaan pembangunan lepas pantai: Strategi pembangunan berkelanjutan di teluk jakarta melalui pembangunan waduk lepas pantai'.

Purnama, S. and Marfai, M. A. (2012), 'Saline water intrusion toward groundwater: Issues and its control', *Journal of Natural Resources and Development* **02**, 25–32.

Qutbudin, I. et al. (2019), 'Seasonal drought pattern changes due to climate variability: Case study in afghanistan', *MDPI Water* **11**(5).

Saleh, L. A. (2018), 'Studying the seepage phenomena under a concrete dam using seep/w and artificial neural network models', *Kerbala, Iraq* .

Stocker, T. F. et al. (2014), 'Working group i contribution to the fifth assessment report of the intergovernmental panel on climate change', *Cambridge University Press* .

Tiyasha, Tung, T. M. and Yaseen, Z. M. (2020), 'A survey on river water quality modelling using artificial intelligence models: 2000–2020', *Journal of Hydrology* **585**, 124670.

Woo, D. L., Young, J. Y., Weon, M. J. and Dong, S. H. (2019), 'Experimental and numerical analysis on hydraulic characteristics of coastal aquifers with seawall', *MDPI Water* **11**(11), 2343.

Zhang, H. et al. (2021), 'Research on seepage field of concrete dam foundation based on artificial neural network', *Alexandria Engineering Journal* **60**, 1–14.

[This page is intentionally left blank]